Contractor-renormalization approach to frustrated magnets in a magnetic field

A. Abendschein* and S. Capponi
Laboratoire de Physique Théorique, Université Paul Sabatier, CNRS, 31062 Toulouse, France
(Received 22 March 2007; revised manuscript received 12 June 2007; published 13 August 2007)

We propose to use the contractor-renormalization (CORE) technique in order to derive effective models for quantum magnets in a magnetic field. CORE is a powerful nonperturbative technique that can reduce the complexity of a given microscopic model by focusing on the low-energy part. We provide a detailed analysis of frustrated spin ladders, which have been widely studied in the past: in particular, we discuss how to choose the building block and emphasize the use of their reduced density matrix. With a good choice of basis, CORE is able to reproduce the existence or not of magnetization plateaux in the whole phase diagram contrary to a usual perturbation theory. We also address the issue of plateau formation in two-dimensional bilayers and point out the analogy between nonfrustrated strongly anisotropic models and frustrated SU(2) ones.

DOI: 10.1103/PhysRevB.76.064413 PACS number(s): 75.10.Jm, 75.60.Ej

I. INTRODUCTION

In the presence of a magnetic field, quantum magnets exhibit fascinating properties. In particular, it can happen that the uniform magnetization along the field exhibits plateaux for rational values, which has given rise to lots of theoretical[1–4] and experimental[5–7] work. The appearance of such plateaux was found to be favored by magnetic frustration.

More recently, experiments on spin dimer compounds (such as $TlCuCl_3$, $KCuCl_3$, and $BaCuSi_2O_6$, see Refs. 8–11) have shown that the triplet excitations behave as bosons that can form superfluid (absence of plateau) or crystalline (finite plateau) phases depending on the competition between repulsive and kinetic interactions. Moreover, the possibility of having both orders, namely, a supersolid, could potentially be observed in related compounds. As is well known, frustration reduces triplet delocalization and, thus, is favorable to a solid behavior, i.e., plateau formation, or supersolid behavior. However, frustrated spin models are difficult to study numerically due to the sign problem of the quantum Monte Carlo (QMC) technique and the absence of reliable large-scale numerical techniques in two dimensions or higher. However, the effective bosonic models themselves can often be simulated when the frustration has disappeared and is absorbed in the effective parameters; indeed, such effective bosonic models have been proposed either based on perturbation theory[2,12,13] or on phenomenological grounds.[14] Therefore, we think that it would be highly desirable to derive nonperturbative effective parameters directly from microscopic models, and we propose to use the contractor-renormalization (CORE) technique to do so.

The CORE method has been proposed in Refs. 15–17 as a systematic algorithm to derive effective Hamiltonians and operators that contain all the low-energy physics. In principle, these effective operators are given by an infinite cluster expansion. CORE has been successfully applied to a variety of both magnetic[17–22] and doped[23,24] low-dimensional systems, and it turns out that, in most cases, the cluster expansion converges quite fast, which is a necessary condition for any practical implementation of this algorithm. Still, the issue about CORE convergence is crucial and currently debated.[25]

In Sec. II, we remind the reader of the CORE algorithm and investigate the frustrated two-leg ladder. Being a well-known model, we can compare our findings to other well-established numerical results and discuss the accuracy of CORE as well as its convergence. In Sec. III, we investigate how to choose the best block decomposition and how to select the low-lying states to keep by using information obtained with the exact reduced density matrix of a block embedded in a large system. Finally, in Sec. IV, we turn to some two-dimensional (2D) bilayer spin models, which are candidates for observing some of these exotic bosonic phases.

II. FRUSTRATED TWO-LEG LADDER

The Hamiltonian $\mathcal{H}$ of the spin $S=\frac{1}{2}$ frustrated antiferromagnetic Heisenberg ladder in an external magnetic field h reads

$$\mathcal{H} = J_\perp \sum_{r=1}^{L} \mathbf{S}_{r,1}\cdot\mathbf{S}_{r,2} + J_x \sum_{r=1}^{L}\sum_{i=1}^{2} \mathbf{S}_{r,i}\cdot\mathbf{S}_{r+1,i} + J_d \sum_{r=1}^{L} (\mathbf{S}_{r,1}\cdot\mathbf{S}_{r+1,2} + \mathbf{S}_{r,2}\cdot\mathbf{S}_{r+1,1}) - h\sum_{r=1}^{L}\sum_{i=1}^{2} S^z_{r,i}. \quad (1)$$

In accordance with Fig. 1, the index $r=1,\ldots,L$ represents the L different rungs of the ladder, whereas $i=1,2$ indicates the two chains that constitute the ladder, and we use periodic boundary conditions along the legs. The rung spin exchange $J_\perp$ is set to 1, while J_x and J_d stand for the interactions along the chain and the diagonal, respectively, which makes the ladder a frustrated system. Note that due to symmetry, J_x and J_d can be interchanged. The role of frustration in the plateau formation can also be understood in a related ladder model.[26]

Throughout this paper, we only consider the physical properties at zero temperature and in the presence of a finite-

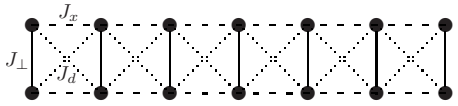

FIG. 1. The spin ladder with coupling $J_\perp$ on vertical rungs, J_x along the legs, and J_d on the diagonal bonds.

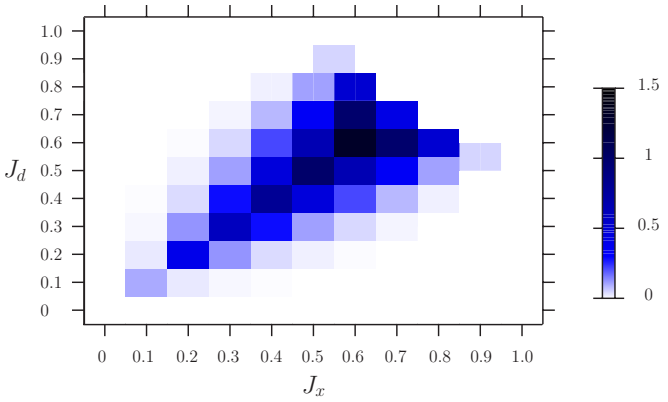

FIG. 2. (Color online) Size of the magnetization plateau at $m_z=\frac{1}{2}m_{sat}$. Results have been obtained after a finite-size scaling analysis of exact diagonalization data obtained on $2\times L$ ladder (up to $L=20$).

magnetic field or, more specifically, the possibility or not of a magnetization plateau at half saturation: $m_z=\frac{1}{2}m_{sat}$.

A. Summary

The frustrated Heisenberg ladder has been studied with various analytical and numerical techniques.[27–29] In the absence of a magnetic field, there are two main regions called the rung singlet phase and the Haldane phase. The effect of a magnetic field has been studied with an exact diagonalization (ED) technique[30] in order to clarify the presence or not of finite-magnetization plateaux. For all the Hamiltonians that we will consider (including the effective ones), S_z^{tot} is a good quantum number; therefore, it is sufficient to compute the ground-state energy in all S_z sectors (in the absence of any magnetic field) and then perform a Legendre transform to get the full magnetization vs field curve $m_z(h)$. We have applied the same ED technique, and we provide in Fig. 2 a sketch of its phase diagram. Data have been extrapolated to the thermodynamic limit after a standard finite-size scaling analysis of the plateau size (see examples in Fig. 3). A large magnetization plateau phase is found around the strongly frustrated

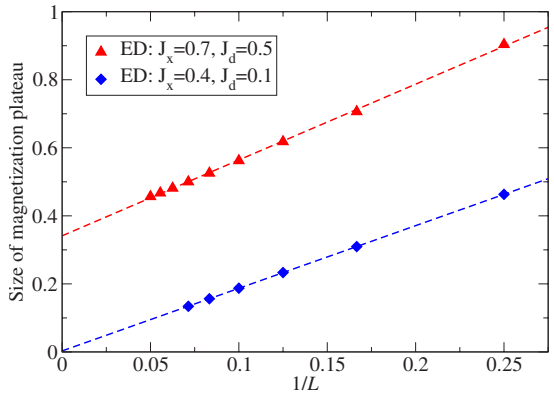

FIG. 3. (Color online) Finite-size scaling of the size of the magnetization plateau at $m_z=\frac{1}{2}m_{sat}$. Data from the numerical exact diagonalization is shown for an example of a finite plateau ($J_x=0.7$ and $J_d=0.5$) and a vanishing plateau ($J_x=0.4$ and $J_d=0.1$).

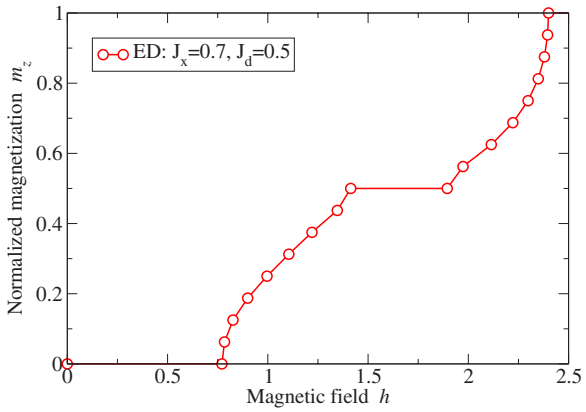

FIG. 4. (Color online) Magnetization m_z along the field (normalized to its saturation value m_{sat}) as a function of magnetic field h on a 2×16 ladder with $J_x=0.7$ and $J_d=0.5$; data from the numerical exact diagonalization has been used.

region $J_x\sim J_d$. We note the existence of different phases without a plateau; in particular, at large $J_d\sim J_x$, there is a first order transition to the so-called Haldane phase.

For the plateau phase, we draw in Fig. 4 a typical magnetization curve obtained on a 2×16 ladder. It exhibits singularities at critical fields[31] and a large half-saturation plateau. Note that in order to mimic the thermodynamic limit, we have drawn a line connecting the middles of the finite-size plateaus of the finite system.

B. Perturbation theory

When the only nonzero coupling is $J_\perp$, the ground state of the ladder is simply the product of singlets on each rung. The states of a given rung are labeled as a singlet $|s\rangle_r=\frac{1}{\sqrt{2}}(|\uparrow\downarrow\rangle_r-|\downarrow\uparrow\rangle_r)$ and the three components of a triplet $|t_{-1}\rangle_r=|\downarrow\downarrow\rangle_r$, $|t_0\rangle_r=\frac{1}{\sqrt{2}}(|\uparrow\downarrow\rangle_r+|\downarrow\uparrow\rangle_r)$, and $|t_{+1}\rangle_r=|\uparrow\uparrow\rangle_r$. In the presence of a finite-magnetic field, due to Zeeman splitting, one can restrict the Hilbert space on each rung to $|s\rangle$ and $|t_{+1}\rangle$, and then do a perturbation theory.[12] Using pseudospin $S=\frac{1}{2}$ operators σ_r for these two states, Eq. (1) can be rewritten as an effective Hamiltonian H_{eff}. Proceeding further, a Jordan-Wigner transformation leads to a system of interacting, one-dimensional (1D), spinless fermions,

$$H_{tV}=t\sum_r^L (c_r^\dagger c_{r+1}+\text{H.c.})+V\sum_r^L n_r n_{r+1}-\mu\sum_r^L n_r, \qquad (2)$$

where t describes the hopping, V the nearest-neighbor interaction, and μ the chemical potential, which can all be expressed in terms of the previously introduced interactions $J_\perp$, J_x, and J_d,

$$t=\frac{J_x-J_d}{2}, \quad V=\frac{J_x+J_d}{2},$$

$$\mu=J_\perp-h. \qquad (3)$$

In the particle language, the occurrence or not of a plateau translates into the existence of a single-particle gap and the

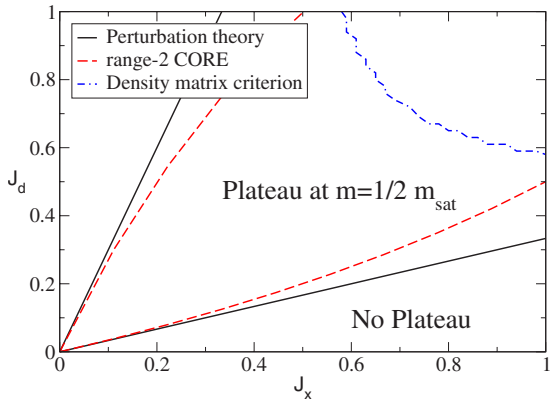

FIG. 5. (Color online) Phase diagram using either perturbation theory or range-2 CORE. Reduced density-matrix calculations on a 2×12 ladder indicate that for large J_x and J_d, the reduced density-matrix weight of the singlet becomes very small while the $S_z=0$ triplet weight increases substantially (region above the blue dash-dotted line, see text for details). For comparison with the exact results, see Fig. 2.

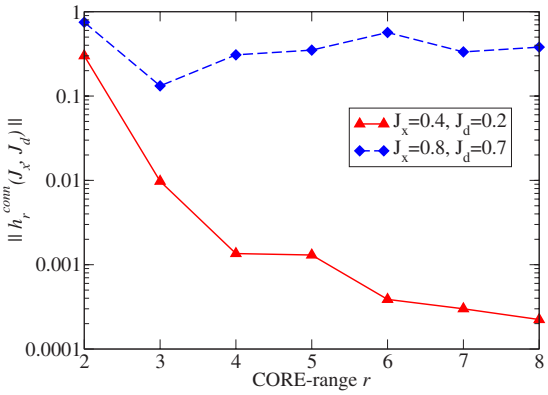

FIG. 6. (Color online) For $J_x=0.4$ and $J_d=0.2$, the norm of h_r^{conn} quickly decreases with increasing range r, whereas for $J_x=0.8$ and $J_d=0.7$, the norm of h_r^{conn} has the same order of magnitude for ranges $2\leqslant r\leqslant 8$.

magnetic field plays the role of an effective chemical potential μ (see Ref. 2). Since the metal-insulator transition of the t-V model[32] occurs at half filling when $V/|t|=2$, we conclude that there will be a finite plateau at half its saturation value when

$$\frac{1}{3} < J_d/J_x < 3. \tag{4}$$

This property is shown in Fig. 5 and reasonably agrees with the exact results of Fig. 2, although we note quantitative differences in the nonperturbative regime. Therefore, we now turn to a nonpertubative CORE approach with the same basis.

C. Contractor renormalization approach in the rung basis

The CORE method has been formulated in 1994 by Morningstar and Weinstein[15,16] and has been used subsequently to study both magnetic systems[17–22] and doped ones.[23,24,33] The idea of this nonperturbative method is to derive an effective Hamiltonian within a truncated basis set, which allows us to reproduce the low-energy spectrum. This means that the original model is replaced by a model with fewer states but a more complicated Hamiltonian under the condition that the retained states of the modified model have an overlap with the set of lowest lying eigenstates of the full original theory.

For clarity, we briefly recall the main CORE steps and refer to the literature for more details. First, one needs to choose a basic cluster and diagonalize it. Then, M low-energy states are kept and the remaining states are discarded. Generally, the M lowest states are retained, but this is not a necessity, as we will discuss in Sec. III. The second CORE step is to diagonalize the full Hamiltonian $\mathcal{H}$ on a connected graph consisting of N_c clusters and obtain its low-energy states $|n\rangle$ with energies ε_n. Third, the eigenstates $|n\rangle$ are projected on the tensor product space of the retained states and Gram-Schmidt orthonormalized in order to get a basis $|\Psi_n\rangle$ of dimension M^{N_c}. Fourthly, the effective Hamiltonian for this graph is defined as

$$h_{N_c} = \sum_{n=1}^{M^{N_c}} \varepsilon_n |\Psi_n\rangle\langle\Psi_n|. \tag{5}$$

Fifthly, the connected range-N_c interactions $h_{N_c}^{conn}$ can be calculated by subtracting the contributions of all connected subclusters. Finally, the effective Hamiltonian is given as a cluster expansion as

$$H^{CORE} = \sum_i h_i + \sum_{\langle ij\rangle} h_{ij}^{conn} + \sum_{\langle ijk\rangle} h_{ijk}^{conn} + \cdots . \tag{6}$$

Then, of course, one has to study this modified effective model, which can still be a difficult task. One possibility is to iterate CORE in the renormalization group spirit and study the properties of its fixed point. Here, following Ref. 20, we propose to check the validity of the effective Hamiltonian *after one step* by comparing its properties to the exact ones on a given finite cluster. Of course, once the effective Hamiltonian has been shown to be accurate, it can be simulated exactly on much larger lattices than the original model, thanks to other numerical techniques. For instance, although the original model is frustrated and cannot be simulated efficiently by QMC, there are cases where the effective Hamiltonian can.

We begin our CORE considerations for the spin $S=\frac{1}{2}$ antiferromagnetic Heisenberg ladder with a rung as a simplest possible basic cluster. Because of the Zeeman splitting, and as in the perturbation approach, we keep only two states per rung: the singlet and the polarized triplet $|t_{+1}\rangle$. Then, we have computed up to range-8 effective CORE interactions by solving exactly up to eight rungs. Despite having an infinite cluster expansion in Eq. (6), previous studies have shown that, in many cases, the long-range effective interactions decay quickly so that they can be neglected beyond a certain range r. This is a necessary condition for any practical implementation of CORE and should be checked systematically.

In Fig. 6, we plot the largest matrix element (in absolute

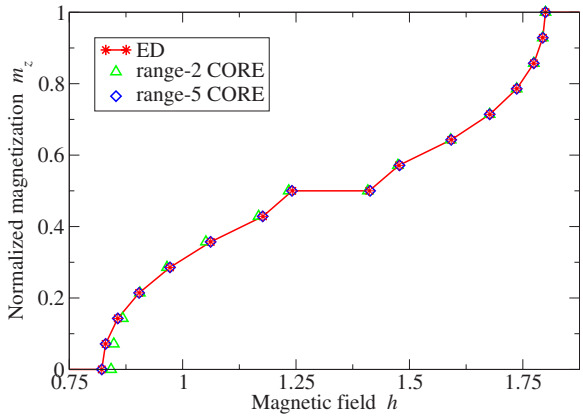

FIG. 7. (Color online) With increasing range, the CORE results converge toward the exact result. Parameters are $2\times L$ with $L=14$; $J_x=0.4$ and $J_d=0.2$. The effective model was obtained up to range 5 and then solved on a 14-site chain.

value) of the range-r connected contribution h_r^{conn}. For the couplings $J_x=0.4$, and $J_d=0.2$, we indeed observe a strong decrease of the amplitudes of the different processes as a function of the range of interaction r. This gives us confidence in the truncation beyond a certain range. However, the case of $J_x=0.8$ and $J_d=0.7$ is an example where this CORE approach does not work, as will be discussed below. Here, the matrix elements of h_r^{conn} remain substantial even for large ranges r.

For the cases where the matrix elements of h_r^{conn} decrease fast with increasing range r, we expect that CORE reproduces the low-energy physics of the system very well. In order to illustrate and strengthen this point, we have *exactly* solved different effective models obtained at a given truncation approximation. In Fig. 7, we show for the example of $J_x=0.4$, and $J_d=0.2$ that with increasing range, CORE results quickly converge to the exact ones.

Since we have used the same basis for CORE as for perturbation theory in Sec. II B, the range-2 effective Hamiltonian will also be a t-V model as in Eq. (2). But for CORE, the dependence of t, V, and μ on the different interactions is different and reads

$$t=\frac{J_x-J_d}{2},\quad V=E_{SS}+\frac{3}{2}J_\perp+\frac{J_x+J_d}{2},$$

$$\mu=-E_{SS}-h-\frac{J_\perp}{2}, \tag{7}$$

where E_{SS} is the ground-state energy of the 2×2 plaquette, which is found to be

$$E_{SS}=-\frac{J_\perp}{2}-\frac{J_x+J_d}{2}-\sqrt{J_\perp^2+J_x^2+J_d^2-J_xJ_d-J_\perp(J_x+J_d)}. \tag{8}$$

Consequently, the condition $V/|t|>2$ for the existence of a magnetization plateau at one-half the saturation value translates into

$$\frac{1}{3-J_x}<J_d/J_x<\frac{3}{1+J_x}. \tag{9}$$

This criterion is shown in Fig. 5 together with the perturbative result. For small interaction J_x, one observes that the plateau phase boundaries given by Eqs. (4) and (9) practically coincide; however, for increasing interaction J_x, i.e., when J_x can no more be treated as a small perturbation, the two curves deviate from each other and CORE becomes more reliable. Note that a range-2 CORE calculation is quite simple, can be done analytically by solving a 2×2 plaquette, and already improves the accuracy with respect to perturbation theory.

The limitations of this approach become evident for $J_x\sim J_d\geqslant 0.7$, where, a naive implementation of CORE fails to reproduce the absence of magnetization plateaux and the matrix elements of h_r^{conn} do not decrease with increasing range r, as shown for $J_x=0.8$ and $J_d=0.7$ in Fig. 6. There is a simple symmetry argument to understand why. For the specific case of $J_x=J_d$, the Hamiltonian has many additional symmetries, namely, the exchange of the two spins on *any* given rung. Therefore, it can be shown that the effective hoppings are strictly zero *at all orders* in the CORE approach, which, of course, leads to a gapped insulating phase at half filling. Indeed, in the CORE algorithm, it is necessary that the ground state has a finite overlap in the reduced Hilbert space.

In the vicinity of the line $J_x=J_d$, this argument is no longer strictly valid but, for practical calculations, we observe that in the CORE calculation, many overlaps become very small, which results in effective models that are not accurate. Even if, in principle, CORE could become accurate if longer-range interactions are taken into account, we think that in such cases, CORE loses its practical utility.

As we will discuss in the following, when the chosen basis does not correctly represent the ground state, practical implementations of the CORE algorithm fail. When this is the case, several strategies are possible: (a) Keep other states for each block, (b) keep more states for each block, or (c) change the block. We now turn to the discussion of each case by focusing on what are the best block decomposition and/or states to keep.

III. CHOICE OF BASIS

CORE will be useful when one can keep a small number of states per block and restrain to finite-range effective interactions. However, checking the convergence is not always easy (except in one dimension as we have shown in Fig. 7), so that it would be useful to have alternative information. In Ref. 20, the authors proposed to used the reduced density matrix of the block as a tool to compute the relative weights of each block state. This procedure is similar to the density-matrix renormalization group method[34] and can help to choose the correct number of kept states or to indicate that a given block decomposition might not be appropriate. Moreover, this analysis can be done independently of CORE since it relies on an *exact* calculation and is rather easy since it can be done on small clusters.[35]

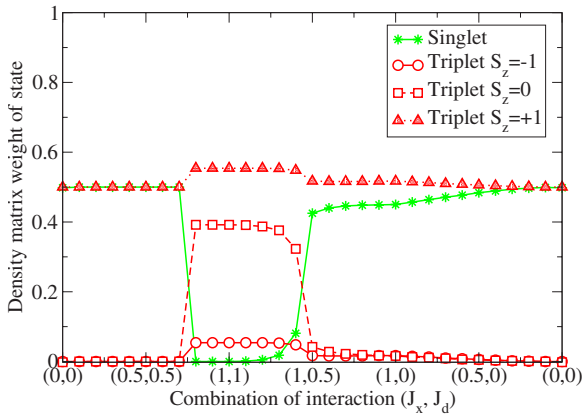

FIG. 8. (Color online) Reduced density-matrix weights for the vertical dimer block obtained on a 2×12 ladder as a function of J_x and J_d along a path in the phase diagram. Calculations have been carried out for a magnetization of $1/2$ of the saturation value.

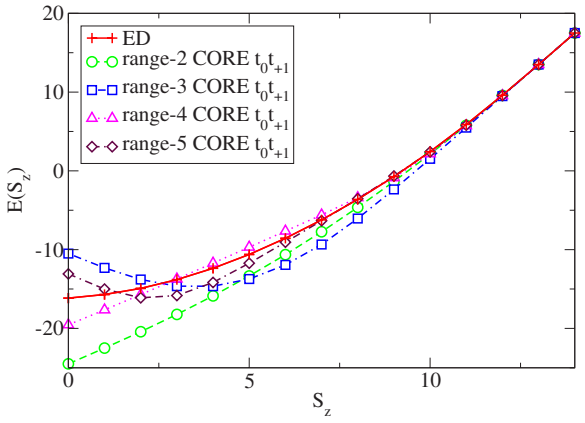

FIG. 9. (Color online) Comparison of energy vs magnetization for $J_x=J_d=1$ on a 2×14 ladder given by ED and various CORE effective Hamiltonians obtained by choosing two triplets on each vertical rung and keeping up to range-r interactions.

A. Rung density matrix

A first illustration of this reduced density-matrix weights is given in Fig. 8. We have considered a rung embedded in a larger cluster, and we trace out the other spins in the exact density matrix obtained with the $m_z=1/2m_{sat}$ ground state[36] (GS) $|\Psi\rangle$. By diagonalizing this reduced density matrix, we obtain the probability of finding a certain block state, given that the overall system has a wave function $|\Psi\rangle$. For our choice of block, we obtain the weights of the rung states, namely, the singlet $|s\rangle$ and the three triplets. We immediately observe that the singlet weight vanishes or is very small when $J_x\sim J_d\geqslant 0.7$, which is precisely the region where a naive CORE calculation fails to reproduce the Haldane phase. In such cases, the exact GS has a vanishing or very small overlap in the naive CORE subspace, which explains the failure of our previous approach.

In Fig. 5, a line indicates the region where the singlet weight becomes smaller than the $S_z=0$ triplet weight. It corresponds precisely to the region with large $J_x\sim J_d$, where exact results have shown that there is no magnetization plateau (see Fig. 2). In this region, one needs to use other strategies for CORE.

B. Keeping two triplets

In most CORE approaches, the kept states have been taken as the lowest in energy in a single block. This choice is, of course, natural and is often the best one. However, in the case where both J_x and J_d are close to $J_\perp$, we will argue that this is not the case. From the reduced density-matrix weight (Fig. 8), we have seen that the rung singlet state does not accurately describe the exact ground state on a large system. Therefore, a first modification to the standard CORE algorithm would be to keep the size of the truncated basis to 2 but to take the largest-weight states, namely, $|t_0\rangle$ and $|t_{+1}\rangle$ in this region (the three-fold degenerate triplets will have a Zeeman splitting in the presence of a magnetic field). As in the previous section, it is straightforward to *analytically* compute the range-2 effective Hamiltonian that has again the form of a t-V model for spinless fermions as in Eq. (2) with

$$t=\frac{J_x+J_d}{2},$$

$$V=\begin{cases} E_{SS}+\dfrac{J_x+J_d-J_\perp}{2} & \text{if } J_x\neq J_d \\ -t & \text{if } J_x=J_d. \end{cases} \tag{10}$$

The crucial difference compared to the perturbative estimate of Eq. (3) is that the effective hopping of polarized triplets *does not vanish* anymore when $J_x=J_d$. As a consequence, this effective mapping correctly predicts that $V/t<2$, so that there is no magnetization plateau.

Of course, we can go beyond the range-2 approximation by including larger clusters in the CORE expansion. In Fig. 9, we consider the highly nonperturbative case where all couplings are equal, and we observe a convergence of the CORE results toward ED data as we increase the range r. However, one needs to take into account longer-range effective interactions in the small-magnetization region, and even for range-5 CORE, the agreement with ED data is not satisfactory.

C. Keeping more states per block

With the rung decomposition, we have observed that CORE is not very efficient if we restrict the truncated basis to singlet and polarized triplet. We have obtained better results by keeping the two dominant triplet states, but the convergence was still poor. The origin of these difficulty lies respectively in (a) the very low density-matrix weight of some states and (b) keeping states that are not the lowest in energy.

To resolve these difficulties, we decide to keep all the rung states, except $|t_{-1}\rangle$. Clearly, if we increase the size of the CORE subspace, we should get more accurate results, but it will limit us in the possibility of studying such an effective model. In Fig. 10, we have numerically solved various effec-

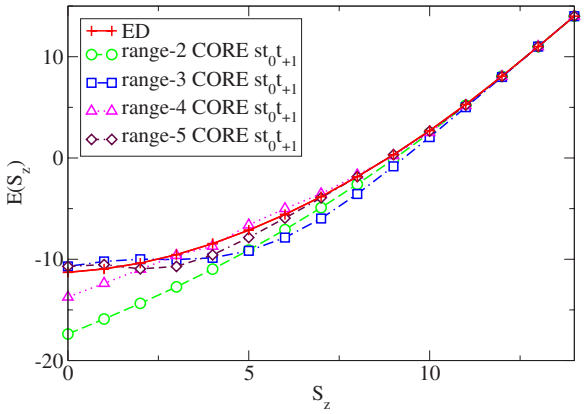

FIG. 10. (Color online) Comparison of energy vs magnetization for $J_x=0.8$ and $J_d=0.7$ on a 2×14 ladder given by ED and various CORE effective Hamiltonians obtained by choosing one singlet and two triplets on each vertical rung and keeping up to range-r interactions.

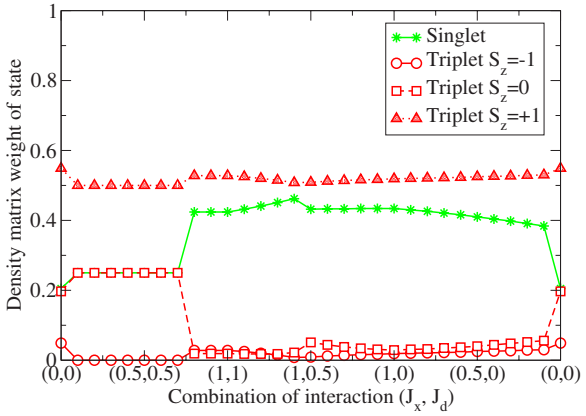

FIG. 11. (Color online) Reduced density-matrix weights for the horizontal dimer block obtained on a 2×12 ladder as a function of J_x and J_d along a path in the phase diagram. Calculations have been carried out for a magnetization of $1/2$ of the saturation value.

tive Hamiltonians obtained by keeping up to a given range r effective interactions. Although qualitatively correct, since we do not observe any finite plateau in this region, the CORE results converge slowly to the exact ones and give poor accuracy at small magnetization.

Note that in the case of $J_x=J_d\geqslant 0.8$, the rung singlet weight vanishes (as shown in Fig. 8), so that the CORE results are identical whether we keep two triplets and the singlet or only two triplets.

As a conclusion for the rung basis, for a given block decomposition, we propose that an efficient CORE implementation should keep the first M low-energy states per block such that the total reduced density-matrix weight is "large." Of course, in some cases, we had to keep a rather large part of the total Hilbert space, which limits us both in numerical simulations and in an analytic a study of the effective model. Therefore, another route can be chosen by modifying the block decomposition.

D. Horizontal dimer block

Since the rung basis does not give accurate results in the strongly frustrated regimes where all three couplings are of the same order, we decide to choose another block decomposition with horizontal dimers, keeping the singlet and polarized triplet: each block will again be represented by a pseudospin $1/2$. Figure 11 illustrates the reduced density-matrix weights of the horizontal dimer states.[36]

By applying CORE, we obtain an effective ladder with many-body effective interactions. In its cluster expansion, the CORE Hamiltonian should, in principle, contain all kind of clusters interactions, including L-shaped ones. However, because we have to deal with *connected* interactions, it can be shown that some cancellations occur: for instance, since a given L-shaped cluster appears in only one rectangular-shaped cluster, its contribution exactly cancels out in the cluster expansion.[37] We have carried out a CORE calculation including up to six-rung interactions, and we have exactly solved these effective models.

In Fig. 12, we compare range-4 and range-6 calculations to exact results when $J_x=J_d=J_\perp=1$. Clearly, the horizontal dimer blocking scheme provides a very good agreement with exact data. In particular, we have a good convergence of CORE data when including longer-range effective interactions. Moreover, although the rung basis wrongly predicted the existence of a magnetization plateau, here, we observe a smooth energy vs magnetization curve and we have checked that there is no indication of any plateau, as is known from exact calculations in this region.

At this stage, by choosing either a two-site rung or leg blocking scheme, we are able to reproduce qualitatively the whole phase diagram for couplings J_x and J_d varying from 0 to $J_\perp$. This gives us confidence that CORE can be used to reduce the complexity of any microscopic model and still gives a correct description of the properties in the presence of a magnetic field. For instance, the effective models that

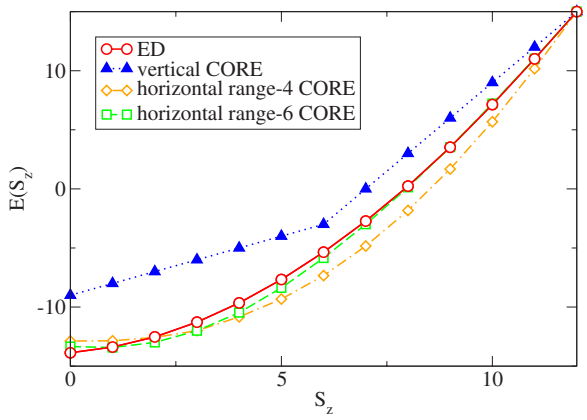

FIG. 12. (Color online) Energy vs magnetization obtained on a 2×12 ladder with isotropic couplings $J_x=J_d=J_\perp=1$. CORE calculations are done with vertical rung blocks, keeping $|s\rangle$ and $|t_{+1}\rangle$ and including *all* effective interactions (corresponds to an infinite range), and horizontal dimer blocks, keeping $|s\rangle$ and $|t_{+1}\rangle$ and including range-4 and range-6 effective interactions. Exact results (ED) are shown for comparison.

we have obtained can be solved exactly on clusters *twice* as large as for the original model.

Because of the large flexibility in the choice of the block, we now turn to another decomposition of the ladder system.

E. Plaquette basis

Another possible block decomposition of a ladder consists of four-site plaquettes. We start the CORE algorithm by classifying its 16 states: two singlets, three triplets, and one quintet. In the presence of a sufficiently strong magnetic field, only the polarized components will be relevant so that we restrict ourselves to six states: the fully polarized quintet $|Q\rangle$, the three fully polarized triplets $|T_A\rangle$, $|T_B\rangle$, and $|T_C\rangle$, and the two singlet states $|S_A\rangle$ and $|S_B\rangle$. In order to make connection with the previous sections, we rewrite those states in terms of the rung basis ones: the polarized quintet state $|S=2,S_z=2\rangle$,

$$|Q\rangle = |t_{+1}t_{+1}\rangle = |t_{+1}\rangle \otimes |t_{+1}\rangle, \quad E_Q = \frac{1}{2}(J_\perp + J_x + J_d);$$

the polarized triplet states $|S=1,S_z=1\rangle$,

$$|T_A\rangle = \frac{1}{\sqrt{2}}(|t_0t_{+1}\rangle - |t_{+1}t_0\rangle), \quad E_{T_A} = \frac{1}{2}(J_\perp - J_x - J_d),$$

$$|T_B\rangle = \frac{1}{\sqrt{2}}(|st_{+1}\rangle - |t_{+1}s\rangle), \quad E_{T_B} = \frac{1}{2}(J_\perp - J_x + J_d),$$

$$|T_C\rangle = \frac{1}{\sqrt{2}}(|st_{+1}\rangle + |t_{+1}s\rangle), \quad E_{T_C} = \frac{1}{2}(J_\perp + J_x - J_d);$$

and the singlet states $|S=0,S_z=0\rangle$,

$$|S_A\rangle = |ss\rangle, \quad E_{S_A} = -\frac{1}{2}(J_\perp + J_x + J_d) - \gamma,$$

$$|S_B\rangle = \frac{1}{\sqrt{3}}(|t_{+1}t_{-1}\rangle + |t_{-1}t_{+1}\rangle - |t_0t_0\rangle),$$

$$E_{S_B} = -\frac{1}{2}(J_\perp + J_x + J_d) + \gamma, \tag{11}$$

where

$$\gamma = \sqrt{J_\perp^2 + J_x^2 + J_d^2 - J_\perp J_x - J_\perp J_d - J_x J_d}.$$

Note that, concerning the energies, the contribution of the magnetic field h has been omitted. Figure 13 shows the behavior of the energies as a function of J_x and J_d along a path in the phase diagram.

We have previously emphasized the use of the reduced density-matrix weights in order to correctly choose which and how many block states should be kept for a given CORE calculation. In Fig. 14(a), we plot the weights of our chosen plaquette states as a function of the ladder couplings (for each state, we compute its weight for all S_z^{tot} and only plot the largest value); therefore, a small value indicates that a given plaquette state is not relevant to describe the exact GS

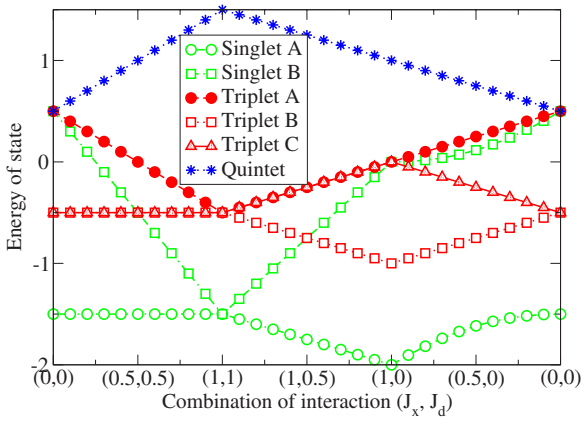

FIG. 13. (Color online) Energy of the plaquette states defined in Eq. (11) as a function of the interaction along the ladder J_x and the diagonal interaction J_d (for $h=0$ and $J_\perp=1$).

for any S_z^{tot}, i.e., for any magnetic field. Using this information, we can even reduce further the CORE basis for some parameters: if some weights are tiny or even zero (typically smaller than 5%), we can reduce the CORE basis from six states to only three (one in each S_z sector) and still have a good accuracy. Of course, reducing the CORE basis allows us to solve exactly the effective model on much larger system sizes (up to 2×36 for the original model). We can also use the reduced density-matrix weights to check whether the six-state basis correctly reproduces exact GS properties: In Fig. 14(b), the total weight of these six states is plotted (we have computed the sum of these six weights for all S_z^{tot} and we only show the smallest value). Since this total weight is larger than 60% in all the phase diagram (couplings and magnetic field), we expect that CORE effective interactions should decay quickly with distance.

Then, by solving exactly the effective models, we can compare the energy vs S_z curve to the exact one. In Fig. 15, we plot our data obtained from various couplings throughout

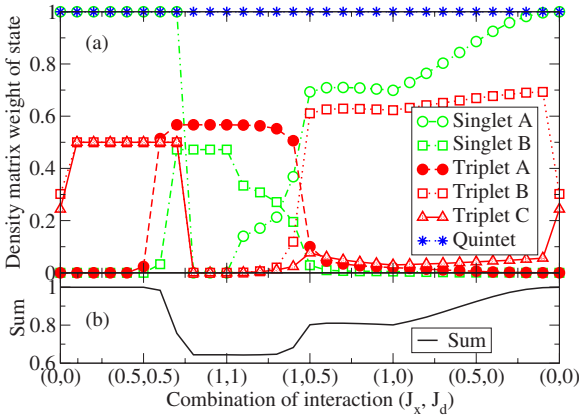

FIG. 14. (Color online) Reduced density-matrix weights of the six chosen plaquette states [see Eq. (11)] as a function of J_x and J_d, obtained by ED from the exact ground state of a 2×12 ladder with various S_z^{tot}: (a) largest weight of the six plaquette states for all S_z^{tot}; (b) minimum over S_z^{tot} of the cumulated weight of the six states. See text for details.

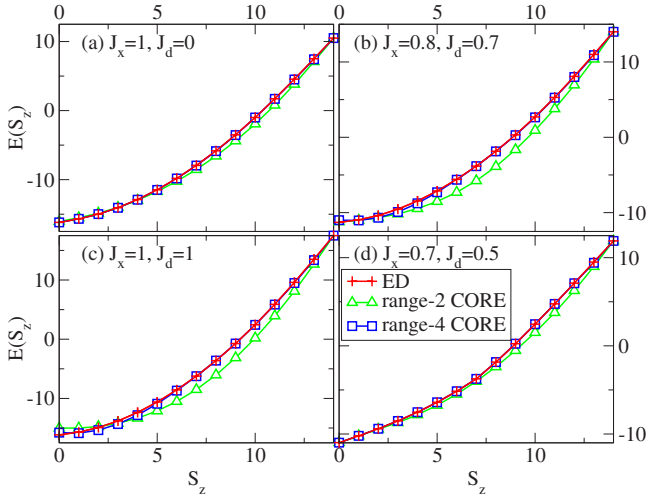

FIG. 15. (Color online) Comparison of energy vs magnetization given by ED and CORE Hamiltonians keeping up to range-2 or range-4 effective interactions for a 2×14 ladder with various couplings. [(a)–(c)] For CORE, we keep only the states per plaquette, which have the largest reduced density-matrix weights (see Fig. 14). (d) For CORE, we keep six states per plaquette [see Eq. (11)].

the phase diagram; CORE calculations are done either with three states (one per S_z sector with the largest reduced density-matrix weight) or all six states according to Fig. 14. In all cases, the CORE convergence is very good and range-4 calculations are very accurate.[38] Being confident in our effective models, we can compute the magnetization curve on much larger systems, and we show in Fig. 16 typical plots showing either the presence or the absence of a magnetization plateau at half saturation, in full agreement with exact results. As a side remark, since our effective models are not necessarily particle-hole symmetric (in the bosonic language), we observe in Fig. 16(a) that the magnetization curve behaves differently close to $m_z\sim 0$ and $m_z\sim m_{sat}$; in particular, the precise shape close to the saturation value converges quite slowly with the range r of the effective CORE interactions.

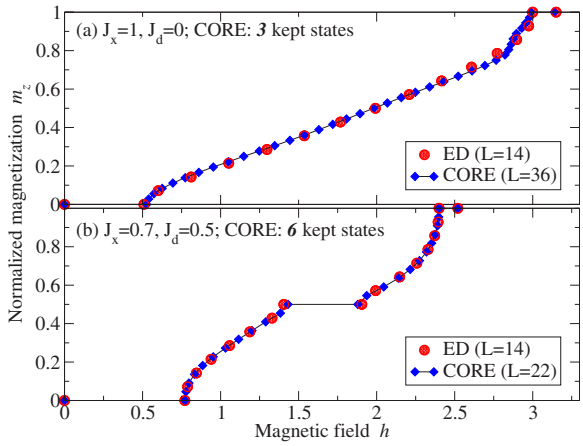

FIG. 16. (Color online) Comparison of magnetization curves for the $2\times L$ ladder obtained with ED and range-3 CORE calculations with (a) three kept plaquette states for $J_x=1$ and $J_d=0$, where there is no plateau, and (b) six kept plaquette states for $J_x=0.7$ and $J_d=0.5$, where there is a finite plateau.

As a conclusion for the frustrated ladder, we have been able to obtain reliable effective Hamiltonians for various block decompositions (vertical or horizontal dimers, or plaquette). For some parameters, some choices are better than the others: for instance, in the nonperturbative frustrated regime where all three couplings are of the same magnitude, we have found that with a plaquette decomposition and keeping only three states per block (not always the low-energy ones), we had a quick convergence of the CORE effective interactions that lead to a high accuracy, while CORE calculations are more difficult starting from rungs. The reduced density-matrix criterion gives us two useful information: (i) It gives a systematic way to locate the energy cutoff and fix how many low-lying states per block should be kept in the CORE approach. (ii) It can also indicate that relevant block states are not necessarily the low-energy ones.

IV. TWO-DIMENSIONAL SYSTEM

A. Anisotropic case

We now consider the 2D bilayer antiferromagnetic spin dimer *XXZ* model which is given by

$$\mathcal{H}_{XXZ} = -h\sum_{\alpha,i} S^z_{\alpha,i} + J\sum_i \mathbf{S}_{1,i}\cdot\mathbf{S}_{2,i} + J'\sum_{\alpha,\langle i,j\rangle}(S^x_{\alpha,i}S^x_{\alpha,j} + S^y_{\alpha,i}S^y_{\alpha,j} + \Delta S^z_{\alpha,i}S^z_{\alpha,j}), \tag{12}$$

where $\alpha=1,2$ denotes the layer index. The interlayer coupling J is the largest one and has an SU(2) symmetry, while the intralayer coupling J is taken with an anisotropy Δ [$\Delta=1$ corresponds to the isotropic SU(2) case]. Such a model has been recently introduced and studied numerically with a QMC technique.[39,40] As for the ladder model, it can be convenient to use the particle language, where the effective triplets behave as hard core bosons that can have a solid (plateau region), a superfluid (no plateau), or even a supersolid phase with both superfluid and solid order parameters. QMC simulations have shown that this model exhibits all these phases,[39] including a large half-saturated magnetization plateau region.

Analogously to the perturbation theory that has been applied on the frustrated two-leg ladder in Sec. II B, we can carry out a perturbation calculation and then derive an effective 2D (hard core) bosonic t-V model,

$$H_{tV} = t\sum_{\langle ij\rangle}(b_i^\dagger b_j + \text{H.c.}) + V\sum_{\langle ij\rangle} n_i n_j - \mu\sum_i n_i \tag{13}$$

or, equivalently, an effective *XXZ* spin-1/2 model. Again, we restrict ourselves to the singlet $|s\rangle$ and the polarized triplet $|t_{+1}\rangle$ on each rung in order to describe the system in a magnetic field close to $m=1/2$.

One finds the following set of parameters:

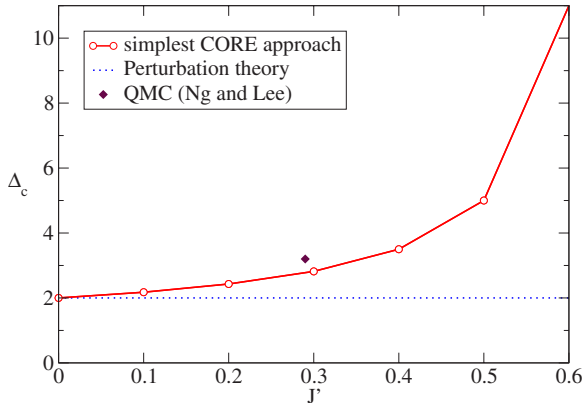

FIG. 17. (Color online) Critical anisotropy Δ_c above which there is a plateau phase as a function of J' for the perturbation theory and the simplest CORE approach for $J=1$. The QMC point, $J'/J=0.29$ and $\Delta_c=3.2$, is taken from Ref. 39.

$$t=\frac{J'}{2},\quad V=\frac{\Delta J'}{2},\quad \mu=J-h. \tag{14}$$

This means that in the perturbation theory, one finds a finite plateau (superfluid-insulator transition) when $V/|t|=\Delta>\Delta_c=2$, which is independent of J and J' (for $J'\neq 0$). This line is drawn in Fig. 17 and deviates from the QMC point.

Performing the simplest CORE approach, we use the same two states ($|s\rangle$ and $|t_{+1}\rangle$). Restricting to range-2 interactions, the parameters for the effective t-V model can be easily derived,

$$t=\frac{J'}{2},\quad V=\frac{\Delta J'}{2}+E_{GS}+\frac{3J}{2},$$

$$\mu=-\frac{J}{2}-E_{GS}-h. \tag{15}$$

Here, E_{GS} is the ground-state energy of the two dimers. We have also calculated the reduced density-matrix weight for this case[36] and observed that the singlet and the polarized triplet represent more than 90% of the total weight in the region of $0\leqslant J'\leqslant 0.5$ and $0\leqslant\Delta\leqslant 4$, which gives us confidence in the reliability of the effective model. We also noted that the weights depend only marginally on J' and Δ (data not shown). For instance, the weights for $\Delta=1$ can be retraced in Fig. 19 in the sector where $J_d=0$.

Comparing with the perturbative result of Eq. (14), one sees that t remains unchanged whereas V and μ are modified. Consequently, the criterion for a superfluid-insulator transition ($V/|t|=2$) is no longer independent of J and J',

$$\frac{V}{|t|}=2=\Delta_c+\frac{2E_{GS}+3J}{J'}. \tag{16}$$

This expression only coincides with the result of the perturbative approach for $J'\to 0$. As shown in Fig. 17, the critical value of the anisotropy Δ_c increases monotonously with J' if we set $J=1$. Above this curve, the CORE approach predicts a solid phase, which means that the system exhibits a magnetization plateau at 1/2 of its saturation value. For comparison, we have added the QMC result[39] indicating a solid phase (i.e., finite plateau) when $J'/J=0.29$ and $\Delta>3.2$, which is remarkably close to our simple estimate. Thus, this CORE approach with two dimers, which is modest and very simple to carry out, is a reliable tool to predict the occurrence of a solid phase and gives a much better agreement with exact results than the perturbation theory.

Moreover, in the numerical study performed by Ng and Lee,[39] a supersolid behavior has been shown to occur close to the solid phase. We believe that it would be desirable to derive effective bosonic models showing such a rich phase diagram, particularly for frustrated models which are not accessible by QMC simulations due to the negative-sign problem. Our simple t-V model of Eq. (2) does not have a supersolid phase but exhibits phase separation instead.[41] For that reason, we extend the range of our CORE approach to range 4; i.e., we consider a system of 2×2 dimers.[42] We then obtain an effective hard core bosonic model containing all possible interactions allowed by symmetry (i.e., conserving the particle number),

$$\begin{aligned}\mathcal{H}=\sum_{i\square_j^k}^{l}\Bigg\{&\frac{C}{N}+\frac{\mu}{4}\Big(\sum_i n_i\Big)+\frac{t_1^{(1)}}{2}(b_i^\dagger b_j+\circlearrowleft+\text{H.c.})+t_1^{(2)}(b_i^\dagger b_k+b_l^\dagger b_j+\text{H.c.})+t_2^{(1)}(b_l^\dagger b_k^\dagger b_i b_j+\text{H.c.})+t_2^{(2)}(b_l^\dagger b_j^\dagger b_i b_k+\circlearrowleft+\text{H.c.})+t_1^{(3)}\\&\times[b_i^\dagger b_l(n_j+n_k-2n_jn_k)+\circlearrowleft+\text{H.c.}]+t_1^{(4)}[b_i^\dagger b_k(n_j+n_l-2n_jn_l)+\circlearrowleft]+\frac{V_2^{(1)}}{2}(n_in_j+\circlearrowleft)+V_2^{(2)}(n_in_k+n_jn_l)\\&+V_3^{(1)}[n_in_j(n_k+n_l-2n_kn_l)+\circlearrowleft]+t_1^{(5)}(b_i^\dagger b_jn_kn_l+\circlearrowleft+\text{H.c.})+t_1^{(6)}(b_i^\dagger b_kn_jn_l+\circlearrowleft)+V_4n_in_jn_kn_l\Bigg\}.\end{aligned} \tag{17}$$

Here, we use the following notation: the sum $\Sigma_{i\square_j^k}^{l}$ goes over the four plaquette sites. The circle $\circlearrowleft$ indicates that all contributions of one kind are included: e.g., $\Sigma_{i\square_j^k}^{l}\left[\frac{t_1^{(1)}}{2}(b_i^\dagger b_j+\circlearrowleft)\right]=\frac{t_1^{(1)}}{2}(b_i^\dagger b_j+b_j^\dagger b_k+b_k^\dagger b_l+b_l^\dagger b_i)$.

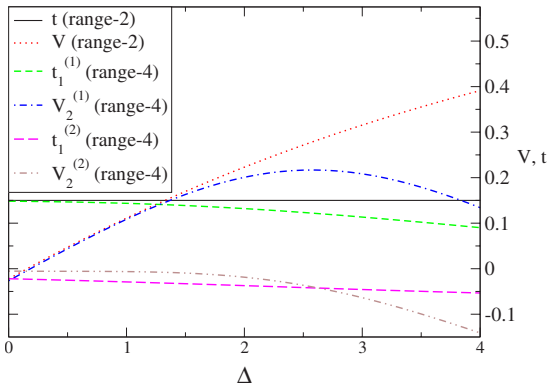

FIG. 18. (Color online) For fixed $J=1$ and $J'=0.3$: t and V as functions of anisotropy Δ for range-2 CORE [see Eq. (15)]; dominant parameters: $t_1^{(1)}$, $t_1^{(1)}$, $V_2^{(1)}$, and $V_2^{(2)}$ also as functions of Δ for range-4 CORE [see Eq. (17)].

In the region of interest, i.e., $J'/J=0.3$ and $0\leqslant\Delta\leqslant 4$, although all parameters are nonvanishing, we find that the dominant terms are the following: the nearest- and next-nearest-neighbor hoppings $t_1^{(1)}$ and $t_1^{(2)}=-t_1^{(6)}$, and the nearest- and next-nearest-neighbor repulsions $V_2^{(1)}$ and $V_2^{(2)}$. The dependence of these parameters on the anisotropy can be seen in Fig. 18 together with the range-2 parameters t and V that have been presented in Eq. (15). For the range-2 data, we note that the transition from the superfluid phase to the solid phase occurs at $\Delta\sim 2.8$ for an interdimer coupling of $J'=0.3$.

Being able to compute a more refined effective Hamiltonian, one could wonder about the possible effects of higher-order terms. This model is very complicated and there is no simple criterion to predict the existence or absence of a plateau phase. Nevertheless, we believe that our range-4 effective Hamiltonian will also possess a plateau phase for large Δ. First of all, since this phase is gapped, we expect it to be robust to small additional interactions. Moreover, starting from a half-filled solid phase, the dominant longer-range terms have the following effect: as shown in Fig. 18, the diagonal density interaction $V_2^{(2)}<0$ enhances the stability of the solid phase, while the diagonal hoppings $t_1^{(2)}$ and $t_1^{(6)}$, which would favor a superfluid phase over the solid, remain small. This qualitative argument could be checked quantitatively by QMC simulations, for instance, with a simpler effective model with no minus-sign problem.

Moreover, the presence of diagonal single-particle hopping $t_1^{(2)}$ and other terms should also stabilize a supersolid phase.[43] In particular, *removing a particle* from the half-filled solid creates a defect that can propagate due to diagonal hopping, which results in a superfluid order parameter coexisting with the solid, i.e., a supersolid. On the contrary, if we *add a particle* to the half-filled solid, our range-4 CORE effective Hamiltonian will not allow for diagonal hopping since the two processes described by $t_1^{(2)}$ and $t_1^{(6)}$ in Eq. (17) will exactly cancel out $(t_1^{(2)}+t_1^{(6)}=0)$. From this observation, we expect that a supersolid phase is stable (unstable) for filling smaller (larger) than 1/2, which is in perfect agreement with the findings of Ref. 39.

It is also interesting to note that among the longer-range effective interactions, correlated-hopping terms could give rise to new phases[14] and could be relevant for some geometries (e.g., the Shastry-Sutherland lattice); here, we have found that their amplitudes remain very small.

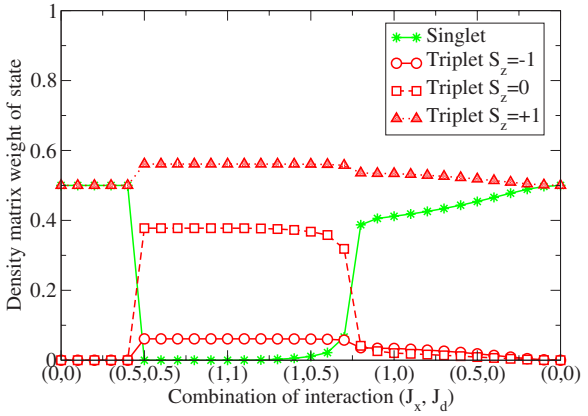

FIG. 19. (Color online) Reduced density-matrix weights for the frustrated 2D Heisenberg bilayer obtained on a 2×16 system as a function of J_x and J_d along a path in the phase diagram. Calculations have been carried out for a magnetization of 1/2 of the saturation value.

B. Frustrated case

Let us now regard the 2D antiferromagnetic bilayer model without anisotropy Δ but with a frustration J_d between the two layers. This system corresponds to the 2D generalization of the frustrated Heisenberg ladder of Eq. (1). Figure 19 illustrates the reduced density-matrix weights.[36]

Carrying out a CORE calculation, we can derive a t-V model on two dimers [see Eq. (13)] or a more complicated hard core boson model including up to four dimer interactions in the form of Eq. (17).

In the range-4 CORE calculation, unlike in the previous anisotropic case, we find that only the nearest-neighbor hopping $t_1^{(1)}$ and repulsion $V_2^{(1)}$ are relevant since the other terms are at least 1 order of magnitude smaller. These parameters are plotted in Fig. 20. Furthermore, one observes that for

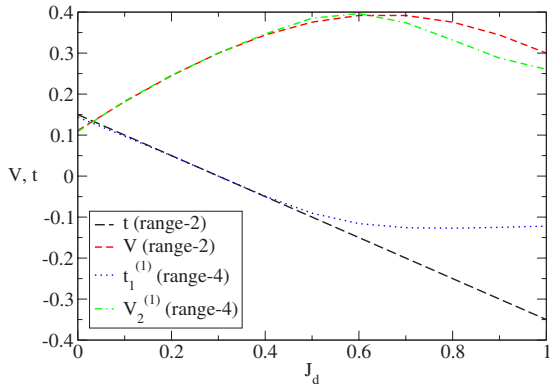

FIG. 20. (Color online) For fixed $J_x=0.3$ in the frustrated case: effective t and V parameters as functions of J_d for range-2 CORE [see Eq. (3)]; $t_1^{(1)}$ and $V_2^{(1)}$ also as functions of J_d for range-4 CORE [see Eq. (17)].

$J_x=0.3$ and $0\leqslant J_d\leqslant 0.5$, the range-2 calculation has already converged; i.e., the effective parameters are almost identical for range-2 and range-4 approximations. Considering the large reduced density-matrix weights of the singlet and the polarized triplet for these parameters (the sum of their contributions exceeds 95% of the total weight, as shown in Fig. 19), we expect that CORE converges fast in this region.

Since the 2D or 1D superfluid-insulator transitions occur when $V/|t|=2$, which corresponds to a frustration of $J_d \sim 0.1$ for $J_x=0.3$, we expect a plateau phase region similar to the one observed in the ladder model (see Fig. 5).

Depending on J_x and J_d values, we find that higher-order terms may become important and could help stabilize a supersolid regime close to the plateau phase. A precise understanding of the effects of these many-body effective interaction is, however, beyond the scope of our study.

V. CONCLUSION

For frustrated ladders, a naive perturbation in the rung basis completely fails to describe the disappearance of plateaux observed for large $J_x\sim J_d\sim J_\perp$. We have shown that even with a simple range-2 CORE calculation keeping two states per rung, which can be done analytically, CORE gives much more accurate boundaries for the plateau region, as seen when comparing exact data from Fig. 2 and CORE predictions in Fig. 5. For the CORE calculations, we have found that it can be crucial to use the information given by the exact reduced density-matrix weights of the kept states in order to choose the best CORE basis, namely, to answer the question: What is the best blocking scheme and how many block states should be kept? Another advantage of the CORE calculation is that its accuracy can be systematically improved by including longer-range effective interactions. By performing various block decompositions and keeping many-body effective interactions, we have shown that CORE is able to reproduce quantitatively the properties of frustrated ladders in the presence of a magnetic field. The reduction of the Hilbert space allows us to exactly solve the effective model on much larger system sizes (up to 2×36) compared to standard ED.

We have also considered two-dimensional anisotropic or frustrated Heisenberg bilayers. In the nonfrustrated anisotropic case, our CORE calculation is improved over the perturbation theory in locating the condition for a plateau formation and is compatible with a recent QMC study. Fine details, such as the occurrence of supersolidity, can also be captured by computing longer-range effective interactions, such as diagonal hopping. In particular, we find that assisted hopping is not a relevant interaction for that geometry and these parameters. The frustrated bilayer was shown to have a similar effective model with similar amplitudes. Therefore, we predict that it will have a similar phase diagram as the anisotropic bilayer, containing superfluid, solid, and supersolid regions. The advantage of such a model is that it respects the SU(2) symmetry and could be more realistic for a material description. Physically, in the anisotropic case, the effective repulsion between hard core bosons increases with growing anisotropy, leading to an insulating phase, whereas in the frustrated case, the effective hopping is also strongly reduced with growing frustration.

ACKNOWLEDGMENTS

We thank IDRIS (Orsay, France) and CALMIP (Toulouse, France) for use of supercomputer facilities. We also thank the Agence Nationale de la Recherche (France) for support. We acknowledge fruitful discussions with F. Alet, N. Laflorencie, and A. Läuchli.

*abendschein@irsamc.ups-tlse.fr

[1] M. Oshikawa, M. Yamanaka, and I. Affleck, Phys. Rev. Lett. **78**, 1984 (1997).
[2] K. Totsuka, Phys. Rev. B **57**, 3454 (1998).
[3] D. C. Cabra, A. Honecker, and P. Pujol, Phys. Rev. B **58**, 6241 (1998).
[4] A. Honecker, J. Schulenburg, and J. Richter, J. Phys.: Condens. Matter **16**, S749 (2004).
[5] H. Kageyama, K. Yoshimura, R. Stern, N. V. Mushnikov, K. Onizuka, M. Kato, K. Kosuge, C. P. Slichter, T. Goto, and Y. Ueda, Phys. Rev. Lett. **82**, 3168 (1999).
[6] H. Kikuchi, Y. Fujii, M. Chiba, S. Mitsudo, T. Idehara, T. Tonegawa, K. Okamoto, T. Sakai, T. Kuwai, and H. Ohta, Phys. Rev. Lett. **94**, 227201 (2005).
[7] Y. Narumi, K. Kindo, M. Hagiwara, H. Nakano, A. Kawaguchi, K. Okunishi, and M. Kohno, Phys. Rev. B **69**, 174405 (2004).
[8] N. Cavadini, C. Ruegg, A. Furrer, H. U. Gudel, K. Kramer, H. Mutka, and P. Vorderwisch, Phys. Rev. B **65**, 132415 (2002).
[9] A. Oosawa, T. Takamasu, K. Tatani, H. Abe, N. Tsujii, O. Suzuki, H. Tanaka, G. Kido, and K. Kindo, Phys. Rev. B **66**, 104405 (2002).
[10] C. Ruegg, N. Cavadini, A. Furrer, H. U. Gudel, K. Kramer, H. Mutka, A. K. Habicht, P. Vorderwisch, and A. Wildes, Nature (London) **423**, 62 (2003).
[11] M. Jaime *et al.*, Phys. Rev. Lett. **93**, 087203 (2004).
[12] F. Mila, Eur. Phys. J. B **6**, 201 (1998).
[13] T. Momoi and K. Totsuka, Phys. Rev. B **62**, 15067 (2000).
[14] R. Bendjama, B. Kumar, and F. Mila, Phys. Rev. Lett. **95**, 110406 (2005).
[15] C. J. Morningstar and M. Weinstein, Phys. Rev. Lett. **73**, 1873 (1994).
[16] C. J. Morningstar and M. Weinstein, Phys. Rev. D **54**, 4131 (1996).
[17] M. Weinstein, Phys. Rev. B **63**, 174421 (2001).
[18] J. Piekarewicz and J. R. Shepard, Phys. Rev. B **56**, 5366 (1997).
[19] E. Berg, E. Altman, and A. Auerbach, Phys. Rev. Lett. **90**, 147204 (2003).
[20] S. Capponi, A. Läuchli, and M. Mambrini, Phys. Rev. B **70**, 104424 (2004).
[21] R. Budnik and A. Auerbach, Phys. Rev. Lett. **93**, 187205 (2004).
[22] P. Li and S. Q. Shen, Phys. Rev. B **71**, 212401 (2005).
[23] E. Altman and A. Auerbach, Phys. Rev. B **65**, 104508 (2002).

[24] S. Capponi and D. Poilblanc, Phys. Rev. B **66**, 180503(R) (2002).
[25] M. S. Siu and M. Weinstein, Phys. Rev. B **75**, 184403 (2007).
[26] A. Honecker, F. Mila, and M. Troyer, Eur. Phys. J. B **15**, 227 (2000).
[27] Zheng Weihong, V. Kotov, and J. Oitmaa, Phys. Rev. B **57**, 11439 (1998).
[28] D. Allen, F. H. L. Essler, and A. A. Nersesyan, Phys. Rev. B **61**, 8871 (2000).
[29] X. Q. Wang, Mod. Phys. Lett. B **14**, 327 (2000).
[30] N. Okazaki, J. Miyoshi, and T. Sakai, J. Phys. Soc. Jpn. **69**, 37 (2000).
[31] I. Affleck, Phys. Rev. B **43**, 3215 (1991).
[32] F. D. M. Haldane, Phys. Rev. Lett. **45**, 1358 (1980).
[33] M. Indergand, A. Lauchli, S. Capponi, and M. Sigrist, Phys. Rev. B **74**, 064429 (2006).
[34] U. Schollwöck, Rev. Mod. Phys. **77**, 259 (2005) and references therein.
[35] Being a local object, we have checked that the local density matrix is rather insensitive to the total size of the system.
[36] Since we focus on magnetization plateau at $m_{sat}/2$, we only show data obtained for $m_z=\frac{1}{2}m_{sat}$ but we have checked that one finds similar results in its vicinity.
[37] E. Altman, Ph.D. thesis, Technion, Israel, 2002.
[38] On a 2×14 ladder, the largest Hilbert space dimension among all S_z^{tot} is 40×10^6 for ED, but only 393 in our CORE subspace obtained by keeping three states per plaquette.
[39] K. K. Ng and T. K. Lee, Phys. Rev. Lett. **97**, 127204 (2006).
[40] N. Laflorencie and F. Mila, Phys. Rev. Lett. **99**, 027202 (2007).
[41] G. G. Batrouni and R. T. Scalettar, Phys. Rev. Lett. **84**, 1599 (2000).
[42] As we have explained in Sec. III D, L-shaped clusters do not give any contribution in the CORE cluster expansion so that only pq rectangles should be considered for the effective interactions (see also Ref. 37).
[43] P. Sengupta, L. P. Pryadko, F. Alet, M. Troyer, and G. Schmid, Phys. Rev. Lett. **94**, 207202 (2005).